

AN ABSTRACT OF THE THESIS OF

Samantha Hemleben for the degree of Master of Science in Robotics presented on March 20, 2017.

Title: Modeling a Spectrum of 3D Printed Materials for Soft Robots

Abstract approved: _____

Yigit Menguc

Soft robotics is an emerging field that heavily relies on the ability of 3D printers. The limitations in soft robotics lie in the area of the 3D printers and the predictive models of the printed materials. There are currently no reliable models for optimizing the gradients required to create soft robots. These gradients are necessary to go from soft to hard materials which are used in electronics and soft robotics grips. This is achievable with the soft materials printed by the Stratasys Objet 500 Connex3, which can print a gradient in materials from hard to soft. Here we show the ability to print a homogeneous gradient on the printer, characterize these homogeneous materials, and model the optimized parameters of the nonlinear elastic material model according to techniques based upon Ogden.

©Copyright by Samantha Hemleben
March 20, 2017
All Rights Reserved

Modeling a Spectrum of 3D Printed Materials for Soft Robots

by

Samantha Hemleben

A THESIS

submitted to

Oregon State University

in partial fulfillment of
the requirements for the
degree of

Master of Science

Presented March 20, 2017
Commencement June 2017

Master of Science thesis of Samantha Hemleben presented on March 20, 2017.

APPROVED:

Major Professor, representing Robotics

Head of the School of Mechanical Industrial and Manufacturing Engineering

Dean of the Graduate School

I understand that my thesis will become part of the permanent collection of Oregon State University libraries. My signature below authorizes release of my thesis to any reader upon request.

Samantha Hemleben, Author

TABLE OF CONTENTS

	<u>Page</u>
1 Introduction	1
1.1 Introduction	1
2 Literature Review	2
3 Materials and Methods	4
3.0.1 Materials	4
3.0.2 Testing the prints	4
3.0.3 Equations	4
3.0.4 Discrete Homogeneous Gradient Modeling	7
3.0.5 Coefficient Modeling	7
4 Results and Discussion	10
4.1 Discussion	10
Bibliography	11

LIST OF FIGURES

<u>Figure</u>	<u>Page</u>
3.1 Tensile test plot for all samples of a) Tango Plus, b) FLX9740, c) FLX9750, d) FLX9760, e) FLX9770, f) FLX9785, g) FLX9795, h) RGD 8430, i) RGD8425, and j) VeroWhite	5
3.2 Tensile test plot with individual Ogden model and coefficient model for all samples of a) Tango Plus, b) FLX9740, c) FLX9750, d) FLX9760, e) FLX9770, f) FLX9785, and g) FLX9795	9
4.1 Extrapolation results for a material between FLX 9750 and FLX 9760.	10

LIST OF TABLES

<u>Table</u>		<u>Page</u>
3.1	Results of Chosen Material Characterizations	6
3.2	Results of Optimized Parameters	8
4.1	Calculated R-Squared values for goodness of fits for each equation.	10

LIST OF ALGORITHMS

<u>Algorithm</u>	<u>Page</u>
1 <i>Fit – Coefficient – Model</i> Pseudo-code illustrating fitting the coefficient model of all materials used.	8

Chapter 1: Introduction

1.1 Introduction

As the field of 3D printing grows in popularity, the need for predictive models of the printed material becomes necessary. The more popular printing materials tend to be hard and have plastic deformation when placed under stress. Recent advances though have allowed for printers to print rubber-like materials that have elastic deformation, specifically the Stratasys Objet 500 Connex3 printer. This printer has the capabilities to print in hard, (Vero), materials and the soft (Tango), materials. For this research Vero White plus and clear Tango Plus were used. The printer also has capability to create a homogeneous gradient of mixes with different percentages of each of the materials varying from hard to soft. These materials in the order of their Young's modulus are Tango Plus, FLX9740, FLX9750, FLX9760, FLX9770, FLX9785, FLX9795, RGD8430, RGD8425, and Vero White. The ability to print these mixes allows for a complete transition from hard to soft in discrete steps within a heterogeneous material sample. Utilizing the capabilities of printing the predetermined homogeneous mixes from Vero White to Tango Plus this paper makes the following contributions:

1. Creating a predictive model for each individual homogeneous material mix sample between the Tango Plus and the Vero White within the gradient according to if they have plastic or elastic deformation. This models the stress of the material for a specific strain value for the materials that act elastically using the Ogden model for non-linear elastic deformation.
2. Creating a coefficient model of each individual homogeneous material mix sample for the Ogden model to predict the coefficients for any percentage of materials mixture based upon the Young's modulus of each material in the printed gradient from Tango Plus to Vero White.

These models allow for better transitions from the hard to soft material while printing on the Stratasys Objet 500 Connex3 by the changes being more predictable. The transitions from hard to soft are necessary while creating soft robots mimicking nature [18], rolling robots that are soft which need hard stabilization points [8], robots with hard electronics [17], and robots with gradients on their outer shell [3]

Chapter 2: Literature Review

A functionally graded material (FGM) is a polymeric material that exhibits varying physical properties due to a heterogeneous material composition [19]. The constituent materials used in the FGM dictate how the FGM will perform overall, therefore the design of the FGM depends largely on material models [10]. Graded polymeric materials have been studied for several decades [13] and remain a continued source for extensive research and development with regards to material modeling and manufacturing [5].

A group from University of Porto used a variety of models to fit experimental data of silicone rubber specimens. Out of the seven models used, they found that Yeoh, Ogden, and Martins models fit the experimental data almost exactly. In this paper, Martin’s model was tested with experimental data for the first time [11]. This research has paved the way for modeling of other hyper elastic materials, which, here, are extended to 3D printing materials.

Researchers at Harvard University have demonstrated that a 3D printed material gradient can offer new advantages in the design of soft robots [18]; for example, a part can be designed to interface between soft and hard structures with varying material composition to achieve compliance that improves energy absorption. Despite this promise, the optimization of a heterogeneous material gradient for soft robotics still requires much more research and optimization.

In addition to individual material models, the design of the complete FGMs depends on the ability to model the material composition of heterogeneous objects as a whole [15]. Jackson et al. [6] showed that it was possible to separate an object into a set of discrete elements made of different materials. Siu et al. [14] introduced a method of spatially assigning material properties within a component, based on proximity to specific geometric features in the component’s design. Dutta et al. [12] demonstrated that material properties could be mapped based on physical simulations of the materials. In order to optimize a part design, Chiu et al. [4] present a method of assigning material distributions based on FEA simulation results. All of these models allow for better understanding of FGMs but no mathematical models exist to illustrate each material and the coefficients used for these materials.

There are many methods for manufacturing FGMs [16], including vapor deposition technique, powder metallurgy and centrifugal methods [9]. But one of the most promising methods is additive manufacturing [4]. Optimization and research has been done in the straight hard to soft intersection of 3D printed materials within the field of additive manufacturing by [7] but there is no mixing of the discrete hard and soft materials. Other studies have pursued a different route and looked at mixing different soft materials using inkjet colored printing (ICP) technology similar to that used in inkjet printers, but still does not mix hard and soft materials [20]. The lack of the mixing of the materials does not allow for optimization of the FGMs.

By combining material modeling, predictive coefficient modeling of materials, and digital manufacturing, new frontiers in multi-material component design can be achieved. This work is the first to present a material model for a set of digitally manufactured photopolymers and to optimize coefficients used in the material models.

Chapter 3: Materials and Methods

3.0.1 Materials

The materials selected to be modeled are the Vero White (hard) and Tango Plus (soft) material (Stratasys). The Connex Objet 500 has the capability to print in a gradient of the homogeneous materials varying from hard to soft based on how much of each material is in the mix. This totaled ten mixtures including pure Tango Plus and Vero White. Tensile testing was performed on all ten materials to create stress strain curves. Then the stress strain data was used to create the models for the materials. This allows for the typical non-linear elastic material models to be compared, due to them being based upon independent strain and dependent stress values. Ogden was the best fit model for the soft material with elastic deformation, and the Young's modulus on the materials that had plastic deformation, and are hard. This is the typical approach difference to plastic and elastic deforming materials because only the linear section of the plastic stress strain curve is considered by calculating the Young's modulus whereas the entire curve until break is considered for elastic deforming materials. The young modulus values are illustrated in table one. These models help predict the wear of the material and the proper coefficients of the model.

3.0.2 Testing the prints

All samples were printed facing the same way on the Connex tray [2] [1]. The support material was removed by hand with no water due to the notice in change of material properties by water. The material was pulled at 1 mm/s in a scaled size of the original specimen of Type IV for test D638 to allow all of the materials to be properly tested on the Mark-10 tensile tester using wedge grips. This material was tested using D638 test because the materials are mixtures of plastic and elastic deforming material and the best representation to have the same test for all is a plastic material test. The dog bones were then tensile tested eight to ten days after they were printed which allowed for full curing of the materials. Tensile testing was done in triplicate for each material mixture, this is shown in figure 3.1. The stress and strain curves lied closely together for the samples of each mixture type. After the stress and strain curve data was generated, the Ogden model coefficients were generated using the materials.

3.0.3 Equations

The simplest stress/strain equation for no lateral stresses is as follows:

$$t_1 = N * k * T(\lambda^2 - 1/\lambda) \quad (3.1)$$

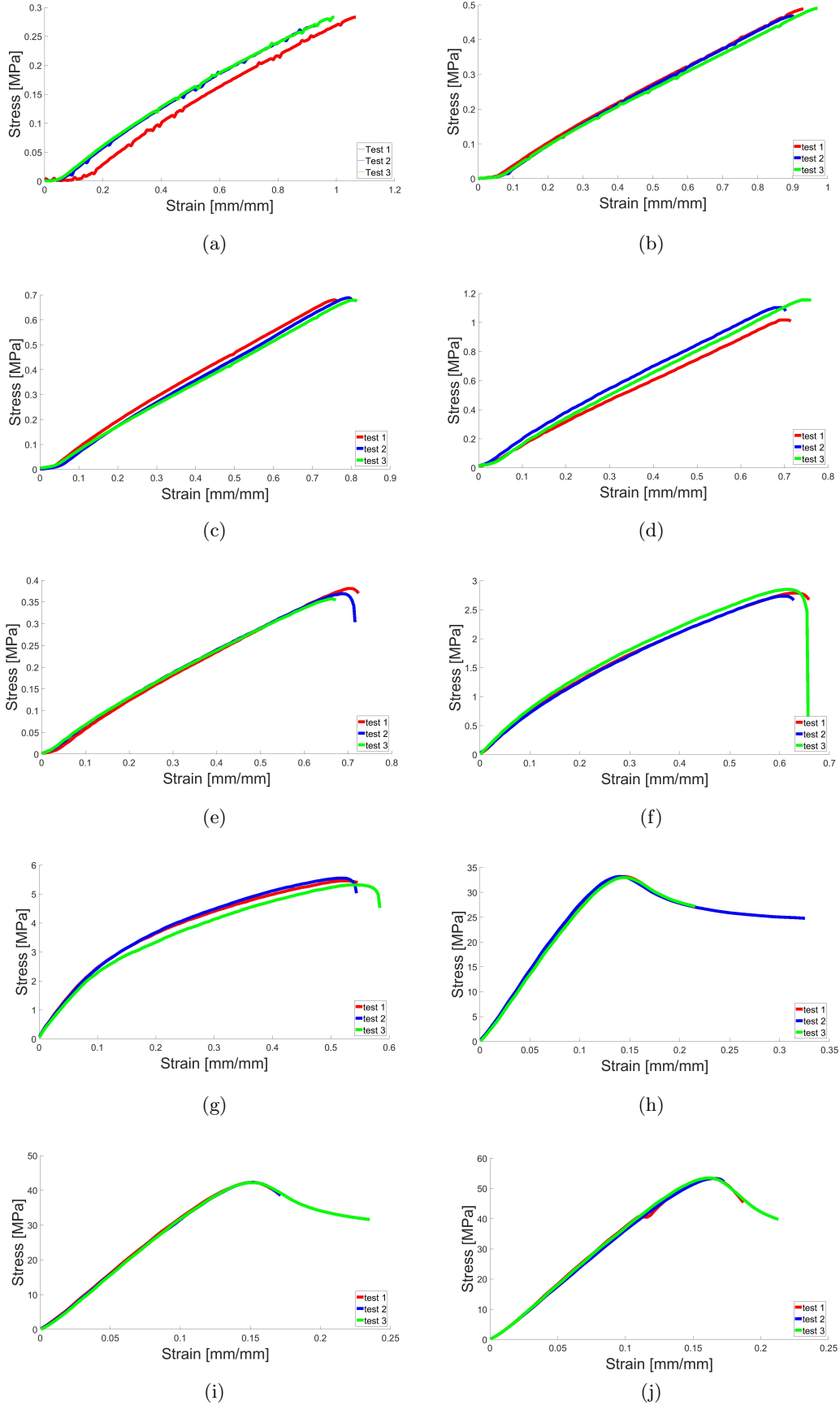


Figure 3.1: Tensile test plot for all samples of a) Tango Plus, b) FLX9740, c) FLX9750, d) FLX9760, e) FLX9770, f) FLX9785, g) FLX9795, h) RGD 8430, i) RGD8425, and j) VeroWhite

Material Type	Youngs Modulus (MPa)	Toughness (kJ/m ³)	Elongation at break (%)
Silicone (Dragonskin 10)	0.087	5.3318	110%
Tango Plus	0.0088	0.0322	100%
FLX 9740	0.0249	0.0347	90%
FLX 9750	0.0141	0.0634	75%
FLX 9760	0.5718	0.0962	70%
FLX 9770	0.3668	0.1437	65%
FLX 9785	2.5499	0.2482	60%
FLX 9795	60.4749	2.1298	55%
RGD 8430	95.5735	5.9956	30%
RGD 8425	159.0943	5.1023	17%
Vero White	342.6460	4.8602	17%

Table 3.1: Results of Chosen Material Characterizations

For equation 3.1, λ is the specified strain at a specific time, t_1 is the stress at that specified strain value, k is Boltzmann's constant, N is the number of chains per unit volume, and T is the absolute temperature based upon using Helmholtz free energy for an isothermal reversible process. The constants are based upon the material type and $N * k * t$ is equivalent to the shear modulus.

The model created by Ogden is based on equation 3.1 and has the general form:

$$W(\lambda_1, \lambda_2, \lambda_3) = w(\lambda_1) + w(\lambda_2) + w(\lambda_3) \quad (3.2)$$

Where the function w is arbitrary, subject to:

$$w(1) = 0, w'(1) + w''(1) = 2\mu$$

where μ is the ground-state shear modulus.

The application of these equations to silicone rubber is shown in equation 3.3:

$$\Omega = \sum_{i=1}^N \frac{c_{(2i-1)}}{c_{2i}} \left[\lambda^{c_{2i}} + 2 \left(\frac{1}{\sqrt{\lambda}} \right)^{c_{2i}} - 3 \right] \quad (3.3)$$

based on [11] where Equation 3.8 was used specifically since $N = 3$ is the number of chains per unit volume for their application.

$$\begin{aligned} \sigma_{Ogden} = c_1(\lambda^{c_2} - 2^{-1+c_2} \lambda^{\frac{-c_2}{2}}) + c_3(\lambda^{c_4} - 2^{-1+c_4} \lambda^{\frac{-c_4}{2}}) \\ + c_5(\lambda^{c_6} - 2^{-1+c_6} \lambda^{\frac{-c_6}{2}}) \end{aligned} \quad (3.4)$$

All resulting equations were based on Equation 3.8 to model the heterogeneous materials that have elastic deformation. The best fit equations using the Matlab optimizer of Levenberg-Marquardt are stated below including their respective parameters, parameter bounds with 95% confidence, and graphs. Equation 3.5 is the equation used in the optimizer for the modeled nine materials.

$$f(\lambda) = c_1(\lambda^{b_1} - 2^{-1+b_1}\lambda^{\frac{-b_1}{2}}) + c_2(\lambda^{b_2} - 2^{-1+b_2}\lambda^{\frac{-b_2}{2}}) + c_3(\lambda^{b_3} - 2^{-1+b_3}\lambda^{\frac{-b_3}{2}}) \quad (3.5)$$

For the remaining heterogeneous materials the Young's moduli's were calculated and shown in Figure 3.1.

3.0.4 Discrete Homogeneous Gradient Modeling

The prints that deformed elastically during the tensile tests were then able to be modeled using a non-linear elastic model. The initial coefficients to be used in the model were created by using Matlab's curve fitting optimizer. The coefficients were then optimized by using Matlab's `fminsearch` function. This allowed for the best possible coefficients of the models for each material individually to be achieved. The model formats and theory are based on [11]. The best fitting models for tango plus and the FLX mixtures were those used for silicone and non-linear elastically deforming materials. Yeoh equation 3.7, Ogden equation 3.8, and Martins equation 3.6 were selected to be tested since they were the best fits for silicone in [11]. Ogden proved to be the best fit with six parameters and resulted in Table 3.2. For the materials that had plastic deformation, their Young's moduli, are found in Table 3.1 during the linear section of their stress strain curve.

$$\sigma_{Martins} = 2(\lambda^2 - \frac{1}{\lambda})c_1c_2e^{c_1(I_1-3)} + 2\lambda(\lambda - 1)c_3c_4e^{c_3(\lambda-1)^2} \quad (3.6)$$

$$\sigma_{Yeoh} = 2(\lambda^2 - \frac{1}{\lambda})(c_1 + 2c_2(I_1 - 3) + 3c_3(I_1 - 3)^2) \quad (3.7)$$

3.0.5 Coefficient Modeling

The creation of the coefficient models was implemented in Matlab. The model illustrates the trend in coefficients as the material mixtures change based on Young's moduli values. The model is implemented by using each materials coefficients for model 3.8, found in the discrete homogeneous gradient modeling. Then the coefficients are fit into a matrix and then two degree polynomial equation with the form $m^2 + m + 1$, where m is the material. Coefficients are solved for so that each equation is able to predict the coefficients as the material changes. The resulting matrix of the

Material	c1	c2	c3	c4	c5	c6
Tango Plus	-0.1546	1.0796	0.5595	0.6907	0.2706	-0.2087
FLX 9740	0.0580	1.4886	0.8032	0.5359	0.4970	-0.4607
FLX 9750	0.0861	-0.5736	1.1267	0.6920	0.9529	-0.2853
FLX 9760	0.0788	-0.0430	1.9908	0.6798	1.6999	-0.3315
FLX 9770	0.0724	-0.0222	3.0960	0.6354	2.5677	-0.3099
FLX 9785	0.0822	-0.0216	5.3104	0.5107	4.0133	-0.2503
FLX 9795	0.2355	-0.0090	11.9248	0.2461	4.0390	-0.1936

Table 3.2: Results of Optimized Parameters

polynomials is processed through iterative least-squares optimization and then Matlab's `fminsearch` function is applied. This fitting process is illustrated in algorithm 1. This model results in figure 3.2 and the below equations:

$$c_1 = -1.1003m^2 + 1.2263m + -0.1408$$

$$c_2 = -0.0046m^2 + -0.5049m + 1.4082$$

$$c_3 = 15.3259m^2 + -5.9351m + 1.0001$$

$$c_4 = -0.7300m^2 + 0.4358m + 0.5459$$

$$c_5 = 3.6022m^2 + 0.8816m + 0.1686$$

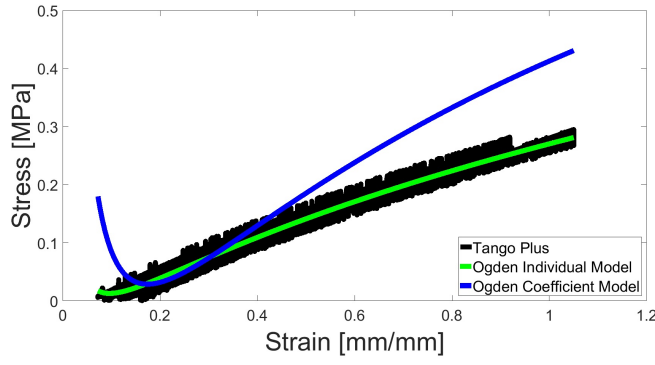
$$c_6 = 0.7538m^2 + -0.6806m + -0.2277$$

which illustrates the trend of coefficients as the material mixture percentage changes for the Ogden model.

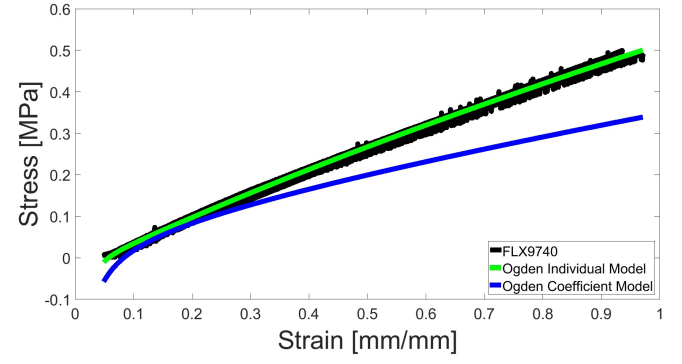
Algorithm 1 *Fit – Coefficient – Model* Pseudo-code illustrating fitting the coefficient model of all materials used.

- 1: **for** each material m_i in M **do**
 - 2: $C0_i \leftarrow \text{Fit-Ogden}(\lambda_i, \sigma_i)$
 - 3: $CF_i \leftarrow \text{fminsearch-SSE}(C0_i, \lambda_i, \sigma_i)$
 - 4: **for** each coefficient c_j in CF^T **do**
 - 5: $A_j \leftarrow \text{Fit-Quadratic}(M, c_j)$
 - 6: **for** each material m_i in M **do**
 - 7: $A \leftarrow \text{fminsearch-SSE}(A, m_i, \lambda_i, \sigma_i)$
-

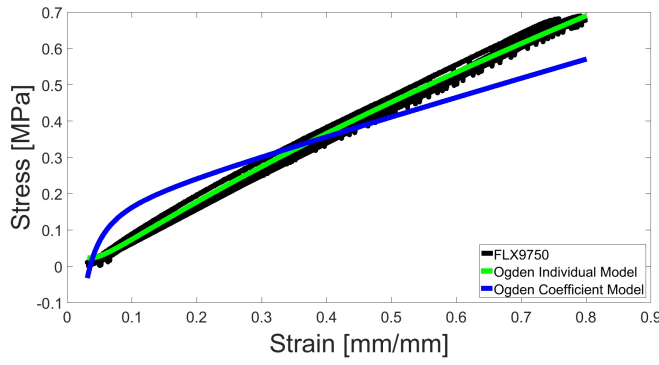
$$\begin{aligned} \sigma_{Ogden} = c_1(\lambda^{c_2} - 2^{-1+c_2}\lambda^{\frac{-c_2}{2}}) + c_3(\lambda^{c_4} - 2^{-1+c_4}\lambda^{\frac{-c_4}{2}}) \\ + c_5(\lambda^{c_6} - 2^{-1+c_6}\lambda^{\frac{-c_6}{2}}) \end{aligned} \quad (3.8)$$



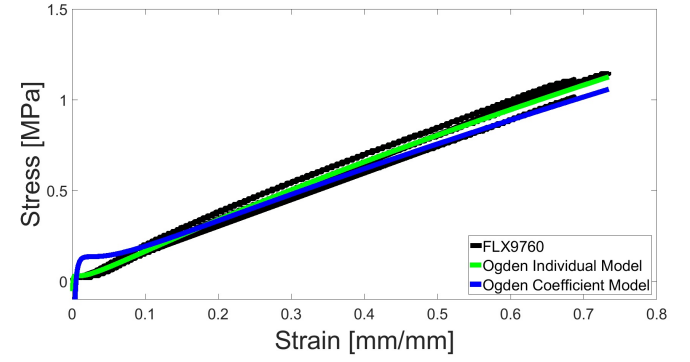
(a)



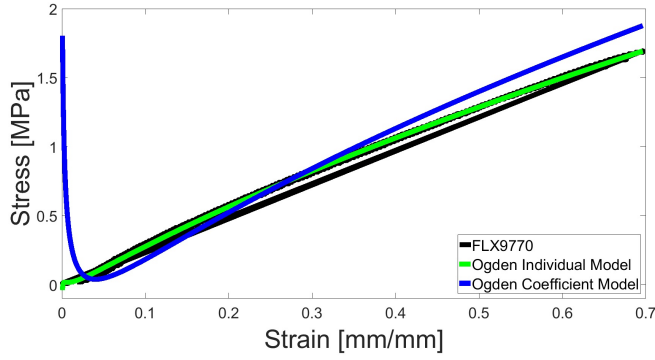
(b)



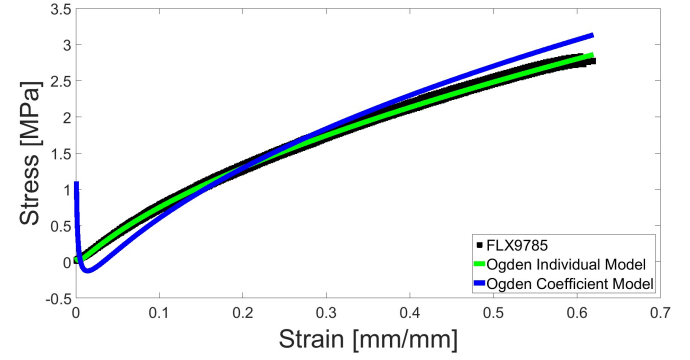
(c)



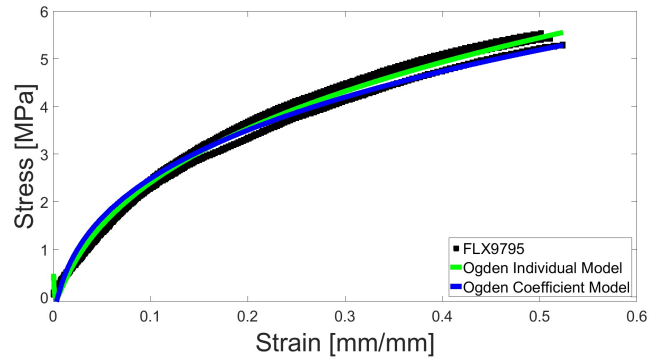
(d)



(e)



(f)



(g)

Figure 3.2: Tensile test plot with individual Ogden model and coefficient model for all samples of a) Tango Plus, b) FLX9740, c) FLX9750, d) FLX9760, e) FLX9770, f) FLX9785, and g) FLX9795

Chapter 4: Results and Discussion

4.1 Discussion

The Ogden model and coefficient model fits well with the printed homogeneous material properties of the gradient from Tango Plus to Vero White. This allows not only for each specific material to be modeled but any new mixtures that may be created. We can see from image 4.1 the coefficient model accurately predicts the stress strain curve for a model for a material between FLX 9750 and FLX 9760. This is due to the model being based upon the Young's modulus. Therefore a new material mixture created on the range of young moduli values currently modeled will also be able to have the coefficients required for that mixture Ogden model. The ability to model not only the materials individually but as a whole allows for better prediction of how 3D printed material wear when placed under strain. This addition of modeling the 3D printed materials to the field allows for the materials to typically be taken from the level of prototyping to allowing them to be used as final products. The use of the printed materials as final products allows for fewer iterations of designs and less wasted material, saving time and money.

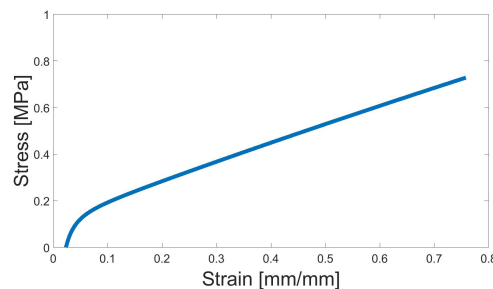


Figure 4.1: Extrapolation results for a material between FLX 9750 and FLX 9760.

Modeling 3D printed materials allows for the advances of the Stratasys Objet 500 Connex3 printer to have further applications than before. Future work can be continued in modeling and

Material	Individual Ogden R-Squared	Coefficient model R-Squared
Tango Plus	0.979939	-0.070096
FLX 9740	0.997883	0.613527
FLX 9750	0.994214	0.877822
FLX 9760	0.987388	0.929626
FLX 9770	0.999212	0.941874
FLX 9785	0.997022	0.945648
FLX 9795	0.990574	0.978788

Table 4.1: Calculated R-Squared values for goodness of fits for each equation.

creating the mixtures that are between the already defined materials in the printer. This will allow for future FGM's to be better optimized and have increased possible applications.

Bibliography

- [1] Stanisław Adamczak, Jerzy Bochnia, and Bożena Kaczmarska. Estimating the uncertainty of tensile strength measurement for a photocured material produced by additive manufacturing. *Metrology and Measurement Systems*, 21(3):553–560, 2014.
- [2] Stanisław Adamczak, Jerzy Bochnia, and Bożena Kaczmarska. An Analysis Of Tensile Test Results to Assess the Innovation Risk for an Additive Manufacturing Technology. *Metrology and Measurement Systems*, 22(1), January 2015.
- [3] Nicholas W Bartlett, Michael T Tolley, Johannes TB Overvelde, James C Weaver, Bobak Mosadegh, Katia Bertoldi, George M Whitesides, and Robert J Wood. A 3d-printed, functionally graded soft robot powered by combustion. *Science*, 349(6244):161–165, 2015.
- [4] W.K. Chiu and K.M. Yu. Direct digital manufacturing of three-dimensional functionally graded material objects. *Computer-Aided Design*, 40(12):1080–1093, December 2008.
- [5] Kai U. Claussen, Thomas Scheibel, Hans-Werner Schmidt, and Reiner Giesa. Polymer Gradient Materials: Can Nature Teach Us New Tricks? *Macromolecular Materials and Engineering*, 297(10):938–957, 2012.
- [6] T. R. Jackson, H. Liu, N. M. Patrikalakis, E. M. Sachs, and M. J. Cima. Modeling and designing functionally graded material components for fabrication with local composition control. *Materials & Design*, 20(2):63–75, 1999.
- [7] Flavia Libonati, Grace X. Gu, Zhao Qin, Laura Vergani, and Markus J. Buehler. Bone-Inspired Materials by Design: Toughness Amplification Observed Using 3d Printing and Testing: Bone-Inspired Materials by Design: Toughness Amplification. . . . *Advanced Engineering Materials*, May 2016.
- [8] Huai-Ti Lin, Gary G Leisk, and Barry Trimmer. Goqbot: a caterpillar-inspired soft-bodied rolling robot. *Bioinspiration & biomimetics*, 6(2):026007, 2011.
- [9] Rasheedat M Mahamood, Esther T Akinlabi, Mukul Shukla, and Sisa Pityana. Functionally graded material: an overview. 2012.
- [10] A. J. Markworth, K. S. Ramesh, and W. P. Parks Jr. Modelling Studies Applied to Functionally Graded Materials. *Journal of Materials Science*, 30(9):2183–2193, 1995.
- [11] PALS Martins, R. M. Natal Jorge, and A. J. M. Ferreira. A Comparative Study of Several Material Models for Prediction of Hyperelastic Properties: Application to Silicone-Rubber and Soft Tissues. *Strain*, 42(3):135–147, 2006.
- [12] Xiaoping Qian and Deba Dutta. Design of heterogeneous turbine blade. *Computer-Aided Design*, 35(3):319–329, 2003.
- [13] M. Shen and M. B. Bever. Gradients in polymeric materials. *Journal of Materials Science*, 7(7):741–746, 1972.

- [14] Y. K. Siu and S. T. Tan. ‘Source-based’ heterogeneous solid modeling. *Computer-Aided Design*, 34(1):41–55, 2002.
- [15] Yan Kit Siu and Sooi Thor Tan. Modeling the material grading and structures of heterogeneous objects for layered manufacturing. *Computer-Aided Design*, 34(10):705–716, 2002.
- [16] Antonella Sola, Devis Bellucci, and Valeria Cannillo. Functionally graded materials for orthopedic applications – an update on design and manufacturing. *Biotechnology Advances*, 34(5):504–531, September 2016.
- [17] Michael T Tolley, Robert F Shepherd, Michael Karpelson, Nicholas W Bartlett, Kevin C Galloway, Michael Wehner, Rui Nunes, George M Whitesides, and Robert J Wood. An untethered jumping soft robot. In *Intelligent Robots and Systems (IROS 2014), 2014 IEEE/RSJ International Conference on*, pages 561–566. IEEE, 2014.
- [18] Deepak Trivedi, Christopher D. Rahn, William M. Kier, and Ian D. Walker. Soft robotics: Biological inspiration, state of the art, and future research. *Applied Bionics and Biomechanics*, 5(3):99–117, December 2008.
- [19] Gururaja Udupa, S. Shrikantha Rao, and K.V. Gangadharan. Functionally Graded Composite Materials: An Overview. *Procedia Materials Science*, 5:1291–1299, 2014.
- [20] Jiwen Wang and Leon L Shaw. Fabrication of functionally graded materials via inkjet color printing. *Journal of the American Ceramic Society*, 89(10):3285–3289, 2006.

